JIPB Journal of Integrative Plant Biology

Research Article
https://doi.org/10.1111/jipb.13660

Knockout of *miR396* genes increases seed size and yield in soybean[oo]

Hongtao Xie[1,2,3†], Fei Su[4†], Qingfeng Niu[1,2†], Leping Geng[1,2], Xuesong Cao[5], Minglei Song[5], Jinsong Dong[4], Zai Zheng[6], Rui Guo[4], Yang Zhang[4], Yuanwei Deng[1,2], Zhanbo Ji[3], Kang Pang[3], Jian-Kang Zhu[5*] and Jianhua Zhu[1,2*]

1. School of Life Sciences, Anhui Agricultural University, Hefei 230036, China
2. Research Center for Biological Breeding Technology, Research Institute of Frontier Science, Anhui Agricultural University, Hefei 230036, China
3. Bellagen Biotechnology Co. Ltd, Jinan 250000, China
4. Institute of Crop Sciences/National Nanfan Research Institute, Chinese Academy of Agricultural Sciences, Key Laboratory of Gene Editing Technologies (Hainan), Ministry of Agriculture and Rural Affairs, Sanya 572025, China
5. Southern University of Science, and Technology, Shenzhen 518055, China
6. Hainan Yazhou Bay Seed Laboratory, Sanya 572024, China
†These authors contributed equally to this work.
*Correspondences: Jian-Kang Zhu (zhujk@sustech.edu.cn); Jianhua Zhu (zhujh@ahau.edu.cn, Dr. Zhu is fully responsible for the distributions of all materials associated with this article)

Hongtao Xie

Jianhua Zhu

ABSTRACT

Yield improvement has long been an important task for soybean breeding in the world in order to meet the increasing demand for food and animal feed. *miR396* genes have been shown to negatively regulate grain size in rice, but whether *miR396* family members may function in a similar manner in soybean is unknown. Here, we generated eight soybean mutants harboring different combinations of homozygous mutations in the six soybean *miR396* genes through genome editing with clustered regularly interspaced palindromic repeats (CRISPR)/CRISPR-associated nuclease (Cas)12SF01 in the elite soybean cultivar Zhonghuang 302 (ZH302). Four triple mutants (*mir396aci*, *mir396acd*, *mir396adf*, and *mir396cdf*), two quadruple mutants (*mir396abcd* and *mir396acfi*), and two quintuple mutants (*mir396abcdf* and *mir396bcdfi*) were characterized. We found that plants of all the *mir396* mutants produced larger seeds compared to ZH302 plants. Field tests showed that *mir396adf* and *mir396cdf* plants have significantly increased yield in growth zones with relatively high latitude which are suited for ZH302 and moderately increased yield in lower latitude. In contrast, *mir396abcdf* and mir396bcdfi plants have increased plant height and decreased yield in growth zones with relatively high latitude due to lodging issues, but they are suited for low latitude growth zones with increased yield without lodging problems. Taken together, our study demonstrated that loss-of-function of *miR396* genes leads to significantly enlarged seed size and increased yield in soybean, providing valuable germplasms for breeding high-yield soybean.

SUMMARY

We created soybean mutants carrying different combinations of mutations in the six *miR396* genes through genome editing with CRISPR/Cas12SF01 in the elite soybean cultivar Zhonghuang 302 and demonstrated that *miR396* genes are negative factors for seed size and loss-of-function of *miR396* genes increased seed size and yield in soybean.

Keywords: Cas12SF01, CRISPR/Cas, *miR396*, seed size, soybean, yield

Xie, H., Su, F., Niu, Q., Geng, L., Cao, X., Song, M., Dong, J., Zheng, Z., Guo, R., Zhang, Y. et al. (2024). Knockout of *miR396* genes increases seed size and yield in soybean. J. Integr. Plant Biol. **00:** 1–11.

INTRODUCTION

Soybean (*Glycine max*) is an important economic crop that provides 28.7% of vegetable oil and 70.7% of protein meal in the world. The demand for food will increase in the future as the global human population continues to grow (Bodirsky et al., 2015). Therefore, increasing yield is an important task in soybean breeding. Soybean yield is influenced by seed weight, which is usually positively associated with seed size (Hu et al., 2023a). Hence, the identification of key genes controlling important agronomic traits, such as seed size, and their utilization in molecular breeding are essential for soybean yield improvement.

Soybean seed traits, including color, shape, and size, are a combination of a series of quantitative traits. Seed size can be described by three main dimensions: length, width, and thickness (Xing and Zhang, 2010). In the past decade, a handful of regulatory genes controlling seed size have been characterized in soybean. *GmCIF1* encodes a cell wall invertase inhibitor; knocking-down of *GmCIF1* through RNA interference (RNAi) increases cell wall invertase activities, leading to heavier seeds (Tang et al., 2017). *GmPLATZ* encoding a zinc-finger transcription factor was identified through transcriptome analyses of developing seeds, and was shown to directly activate the expression of *GmGA20OX* and cyclin genes to enhance soybean seed size and weight (Hu et al., 2023a). Through co-expression network analysis, *GmJAZ3* was identified as a seed development regulator, and the GmJAZ3-GmRR18a-GmMYC2a-GmCKXs module promotes seed size by orchestrating jasmonate and cytokinin signaling (Hu et al., 2023b). *GmPDAT* was identified through genome-wide association studies (GWAS) as a seed size regulator, and subsequent research revealed that overexpression of this gene increased seed size, whereas knockdown of the gene through RNAi decreased seed size (Liu et al., 2020). Overexpression of *GmMFT* increased seed weight, whereas its mutants exhibited decreased seed weight (Cai et al., 2023). A study on soybean domestication revealed that *GmSWEET10a* and *GmSWEET10b* promote seed size through increasing seed sugar and oil contents while reducing protein content (Wang et al., 2020). The identification of additional genes regulating seed size will facilitate molecular breeding for yield improvement in soybean.

miR396 is one of the most evolutionarily conserved micro RNA (miRNA) families in monocots and eudicots. In Arabidopsis, *miR396* controls seed size by post-transcriptionally repressing its target genes, the *GROWTH REGULATING FACTORS* (*GRFs*) (He and Hannon, 2004; Jones-Rhoades et al., 2006). Overexpression of the *miR396* target genes *AtGRF1*, *AtGRF2* and *AtGRF5* in Arabidopsis leads to bigger seeds (Van Daele et al., 2012). Natural *GL2/GS2* alleles were identified that correspond to *OsGRF4* with two-point mutations at the *miR396* binding site; the mutations relieve *OsGRF4* from repression by *miR396*, so that OsGRF4 can activate brassinosteroid response to increase grain size, resulting in grain yield increase (Che et al., 2015; Duan et al., 2015; Hu et al., 2015; Li et al., 2016). In addition, target mimicry of *OsmiR396b* (MIM396) allowed elevated expression of its target gene *OsGRF6*, leading to improved grain yield by enhancing the development of auxiliary branches and spikelets (Gao et al., 2016). Furthermore, the simultaneous knockdown of *miR396e* and *miR396f* in rice through genome editing increased grain size and panicle branching, leading to increased grain yield, especially under nitrogen-deficient conditions (Miao et al., 2020; Zhang et al., 2020). Although biological functions of the *miR396-GRF* module have been described in Arabidopsis and rice, whether *miR396* family genes may function in a similar manner in soybean remains unknown.

The recently developed clustered regularly interspaced palindromic repeat (CRISPR)/CRISPR-associated nuclease (Cas) 12SF01 is a highly effective gene editing system in plants and animals (Lv et al., 2024; Duan et al., 2024). In this study, through systematically mutating the six *miR396a/b/c/d/f/i* genes in soybean, we found that the seed length, width, and thickness of *mir396* mutants were all significantly increased. We further showed that the *mir396adf* and *mir396cdf* plants have increased yield and are suited to grow in ecological zones at relatively high latitude, whereas the *mir396abcdf* and *mir396bcdfi* plants show increased yield when cultivated in lower latitude ecological zones. Thus, *miR396* was found to be an important negative regulator of seed size and yield in soybean, making its knockout mutants valuable germplasms for breeding high-yielding soybean varieties.

RESULTS

Precise gene editing of soybean *miR396* family members using CRISPR/Cas12SF01

The soybean genome contains six *miR396* genes (*miR396a*, *miR396b*, *miR396c*, *miR396d*, *miR396f* and *miR396i*) (Figure S1). Sequence analyses show that *miR396a/i* have similar sequences, while *miR396b/c/d/f* are similar (Figure 1A). To dissect the function of the *miR396* genes in soybean, we constructed a dual single guide RNA (sgRNA)-expression CRISPR/Cas12SF01 vector with CRISPR RNA (crRNA1) targeting *miR396a/i* and crRNA2 targeting *miR396b/c/d/f* (Figure 1B). The vector was transformed into the soybean cultivar Zhonghuang 302 (ZH302), an elite cultivar widely grown in the Huang-Huai River basin and southern region of China. From the T_1 to T_3 generations, we identified eight homozygous mutant lines for the six *miR396* family members: *mir396aci*, *mir396acd*, *mir396adf*, *mir396cdf*, *mir396abcd*, *mir396acfi*, *mir396abcdf*, and *mir396bcdfi*. These mutant plants contain deletion mutations in the corresponding *miR396* family members (Figures 1C, D, S2).

The *mir396* mutants produce bigger seeds in Shandong

Because ZH302 is mostly suited for cultivation in growth zones between the Huang (Yellow) River and Huai River and southern part of China, we evaluated the performance of the *mir396* mutants in one of the provinces in this region, Jinan of

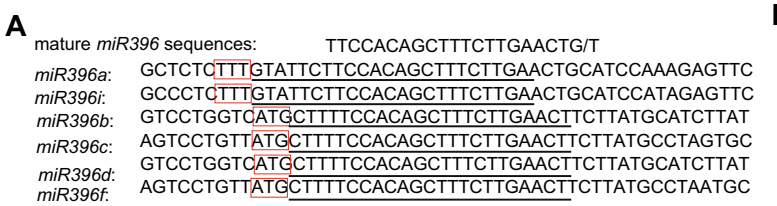

C

Mutant Type	Variety	*miR396a*	*miR396b*	*miR396c*	*miR396d*	*miR396f*	*miR396i*
mir396aci	ZH302	-5 bp	WT	-26 bp	WT	WT	-2 bp
mir396acd	ZH302	-5 bp	WT	-2 bp	-11 bp	WT	WT
mir396adf	ZH302	- 1 bp	WT	WT	-11 bp	-1 bp	WT
mir396cdf	ZH302	WT	WT	-26 bp	-1 bp	-2 bp	WT
mir396abcd	ZH302	-5 bp	-1 bp	-2 bp	-11 bp	WT	WT
mir396acfi	ZH302	-5 bp	WT	-26 bp	WT	-1 bp	-2 bp
mir396abcdf	ZH302	-5 bp	-69 bp	-26 bp	-11 bp	-2 bp	WT
mir396bcdfi	ZH302	WT	-3 bp	-2 bp	-9 bp	-2 bp	-2 bp

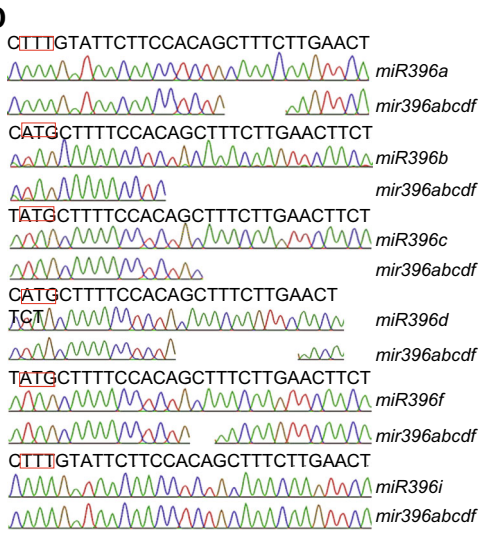

Figure 1. Targeted mutation of *Gma-miR396a/b/c/d/f/i* genes by clustered regularly interspaced palindromic repeats (CRISPR)/CRISPR-associated nuclease (Cas)12SF01

(A) CRISPR RNA (crRNA) target sites for *miR396a/i* and *miR396b/c/d/f* members. The crRNA sequences are underlined, and the protospacer-adjacent motif (PAM) sequences are marked with red boxes. **(B)** Schematic illustration of the CRISPR/Cas12SF01 binary vector. *pAtU6*, *AtU6* promoter; *pGmU6*, *GmU6* promoter; *pSlEF1α*, *SlEF1α* promoter (*Solyc06g005060.2.1*); HDV, self-cleaving ribozyme; E9t, terminator. **(C)** Genotypes of homozygous *mir396* mutants generated in the ZH302 background. **(D)** Sanger sequencing of the *mir396abcdf* mutant. The PAM sequences are marked with red boxes.

Shandong Province, China. We found that the plant height was increased by 6.0% and 10.9% in the *mir396abcdf* and *mir396bcdfi* plants, respectively (Figure 2A, B). All the *mir396* mutants had similar numbers of nodes on the main stems as the ZH302 (Figure 2C). It is apparent that plants of all the *mir396* mutants had more branches than the ZH302 plants, and plants of the *mir396adf*, *mir396cdf* and *mir396abcd* mutants produced more total pods per plant as well as more effective pods per plant than the ZH302 plants (Figure 2D–F). Interestingly, the number of seeds per plant was increased by 14.7% for *mir396adf*, but was decreased by 13.1% and 17.8% in the *mir396abcdf* and *mir396bcdfi*, respectively (Figure 2G). Importantly, we found that all of the *mir396* mutants had larger seeds than those from ZH302 plants, with an average increase of 7.6%, 6.4%, and 3.8% in seed length, width, and thickness, respectively, resulting in an 10.3% increase in 100-seed weight (Figure 2H–K). In the *mir396acd*, *mir396adf*, and *mir396cdf* mutants, the seed length was 6.1%, 4.8%, and 4.7% greater (Figure 2H), seed width was 5%, 5%, and 3.5% greater (Figure 2I), and seed thickness was 3.2%, 2.7%, and 1.9% greater (Figure 2J), resulting in a 9.3%, 9.1%, and 4.2% increase in 100-seed weight, respectively (Figure 2K). In addition, the *mir396acd*, *mir396adf* and *mir396cdf* mutants had an average of 3.9%, 10.2%, and 9.6% increase, respectively, in yield per plot compared with ZH302 plants (Figure 2L). Although the *mir396abcdf* and *mir396bcdfi* mutants had the largest increases in seed length (11.6% and 19.0%), width (7.3% and 14%), thickness (4.7% and 6.9%), and 100-seed weight (14.5% and 22.4%), respectively, compared with ZH302 plants (Figure 2H, K), the yield per plot was actually decreased by 8.8% and 8.4%, respectively, compared with ZH302 plants (Figure 2L). It is worth noting that the *mir396abcdf* and *mir396bcdfi* mutants had significant lodging problems at late growth stages, which may explain, at least partially, the yield decrease.

Because we observed a yield increase in the triple mutant *mir396adf* and a decrease in yield in the quadruple mutant *mir396abcdf* grown in Jinan in 2022, we re-evaluated the performance of these two mutant plants in the same field in 2023. The *mir396abcdf* plants were taller than ZH302 plants (Figure 3A, F). Both the *mir396adf* and *mir396abcdf* plants produced similarly shaped pods as the ZH302 plants, but they had bigger seeds than the ZH302 plants (Figure 3B–E). Although the *mir396adf* and *mir396abcdf* plants produced similar numbers of nodes on the main stems as ZH302 (Figure 3G), they had more branches and total pods per plant than ZH302 (Figure 3H, I). The *mir396adf* plants, but not the *mir396abcdf* plants, had more effective pods per plant than ZH302 (Figure 3J). Compared with ZH302, the *mir396adf* plants had increased yield whereas the *mir396abcdf* plants had decreased yield due to lodging (Figure 3K). We also determined the protein and oil contents in the seeds of *mir396adf* and *mir396abcdf* plants and found that they had decreased protein contents, but increased oil contents (Figure 3L, M). Overall, these results are consistent with the data collected from the *mir396adf* and *mir396abcdf* plants grown in this region from the previous year.

Plants of the *mir396* mutants produce bigger seeds in Hainan

While multiplying the seeds in Sanya of Hainan Island during the winter season in 2022, we evaluated the performance of *mir396* mutants in this region (Figure 4A). In Sanya, the plant height was increased by 7.6%, 8.1%, 19.7%, 26.4%, and

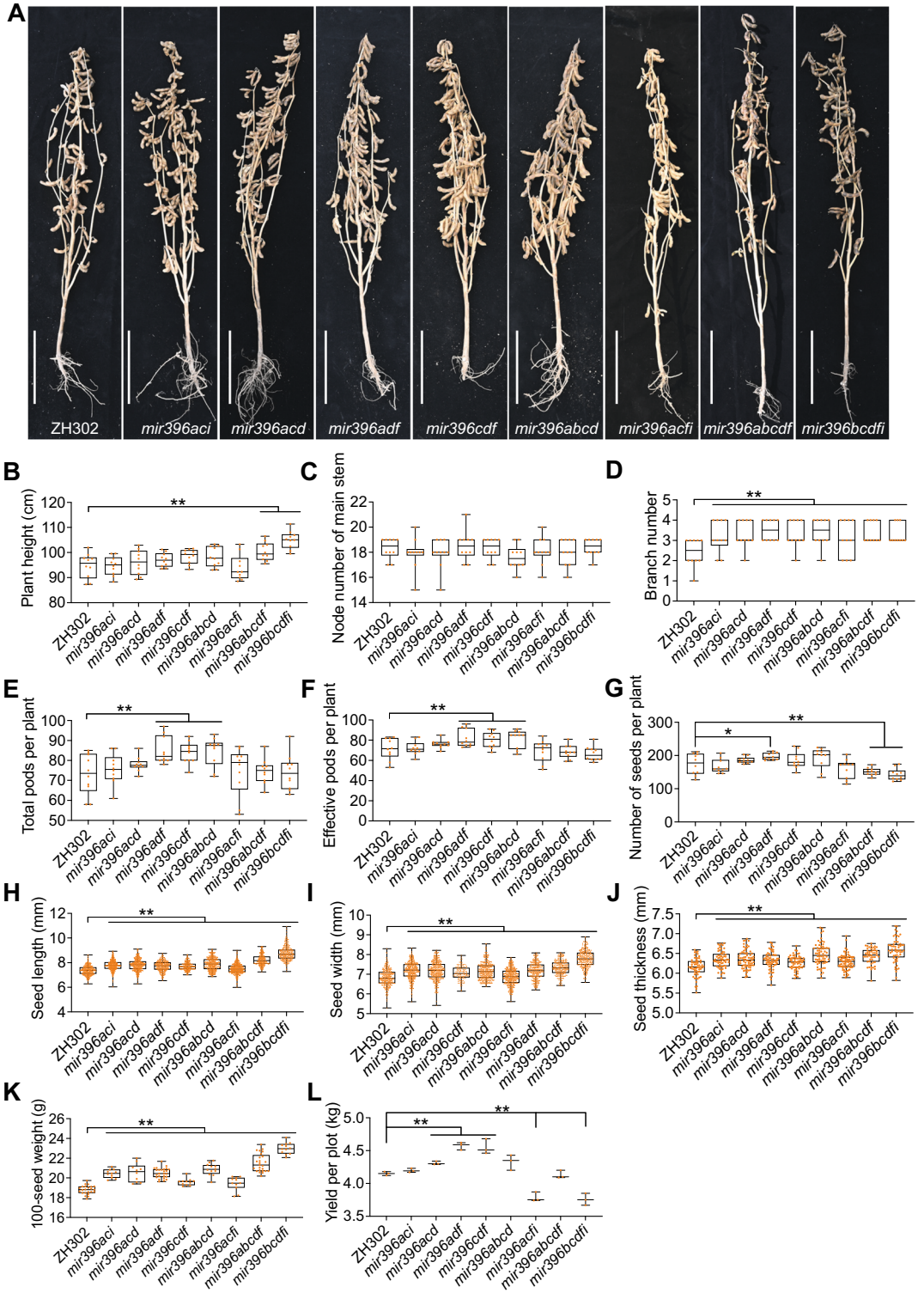

Figure 2. Phenotypic analysis of the *mir396* mutants in Shandong in 2022

(A) Morphology of ZH302 and *mir396* mutants at mature stage. Bar = 25 cm. **(B–L)** Quantification of the plant height **(B)**, node number of main stem **(C)**, branch number **(D)**, total pods per plant **(E)**, effective pods per plant **(F)**, number of seeds per plant **(G)**, seed length **(H)**, seed width **(I)**, seed thickness **(J)**,100-seed weight **(K)** and yield per plot **(L)** of ZH302 and *mir396* mutants. Data are means ± *SD* ($n = 10$–18 in **B**-**G**, 100–280 in **H**–**J**, 11–25 in **K** and three in **L**). Two-tailed Student's *t*-tests were used for statistical analysis. Asterisks indicate significant differences compared with ZH302 (*$P < 0.05$; **$P < 0.01$).

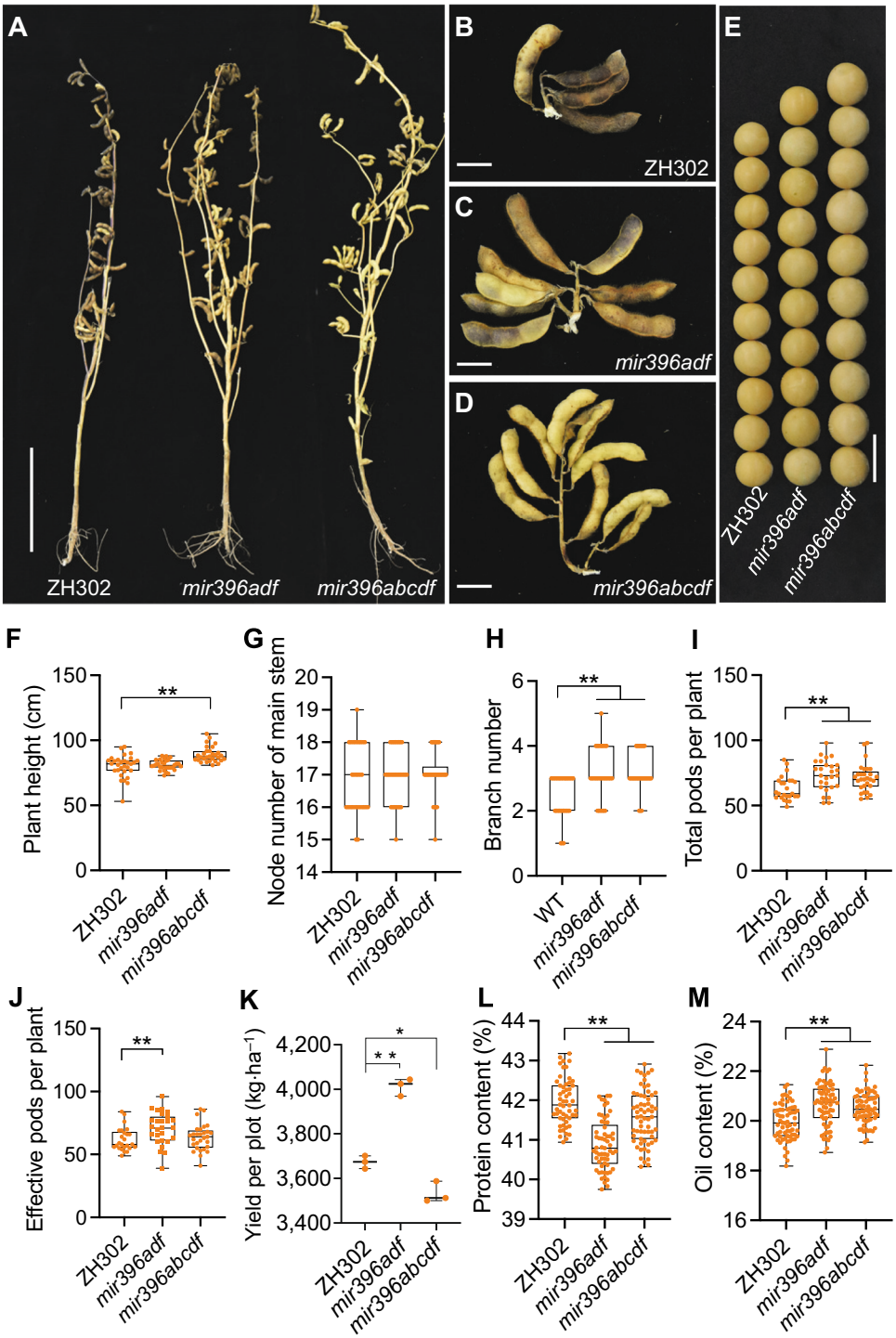

Figure 3. The *mir396adf* and *mir396abcdf* mutations improve soybean field productivity in Shandong in 2023

(A–E) Morphology **(A)**, pods **(B–D)**, and seeds **(E)** of ZH302, *mir396adf*, and *mir396abcdf* plants at mature stage. Bar = 20 cm (plant height), 2 cm (pod), and 1 cm (seed size). **(F–M)** Quantification of the plant height **(F)**, node number of main stem **(G)**, branch number **(H)**, total pods per plant **(I)**, effective pods per plant **(J)**, yield per plot **(K)**, seed protein content **(L)** and oil content **(M)** of ZH302, *mir396acd* and *mir396abcdf*. Data are means ± *SD* ($n = 25–29$ in **F–J**, three in **K** and 54–67 in **L**, **M**). Two-tailed Student's *t*-tests were used for statistical analysis. Asterisks indicate significant differences compared with ZH302 (*$P < 0.05$; **$P < 0.01$).

23.4% in the *mir396acd*, *mir396cdf*, *mir396abcd*, *mir396abcdf*, and *mir396bcdfi*, respectively, but was not significantly altered in the *mir396aci*, *mir396adf*, and *mir396acfi* mutants compared to ZH302 (Figure 4C). As observed in Shandong, the number of nodes on the main stems did not change in any of the *mir396* mutants (Figure 4D), suggesting that the increased overall plant height in the *mir396acd*, *mir396cdf*, *mir396abcd*, *mir396abcd*, *mir396abcdf*, and

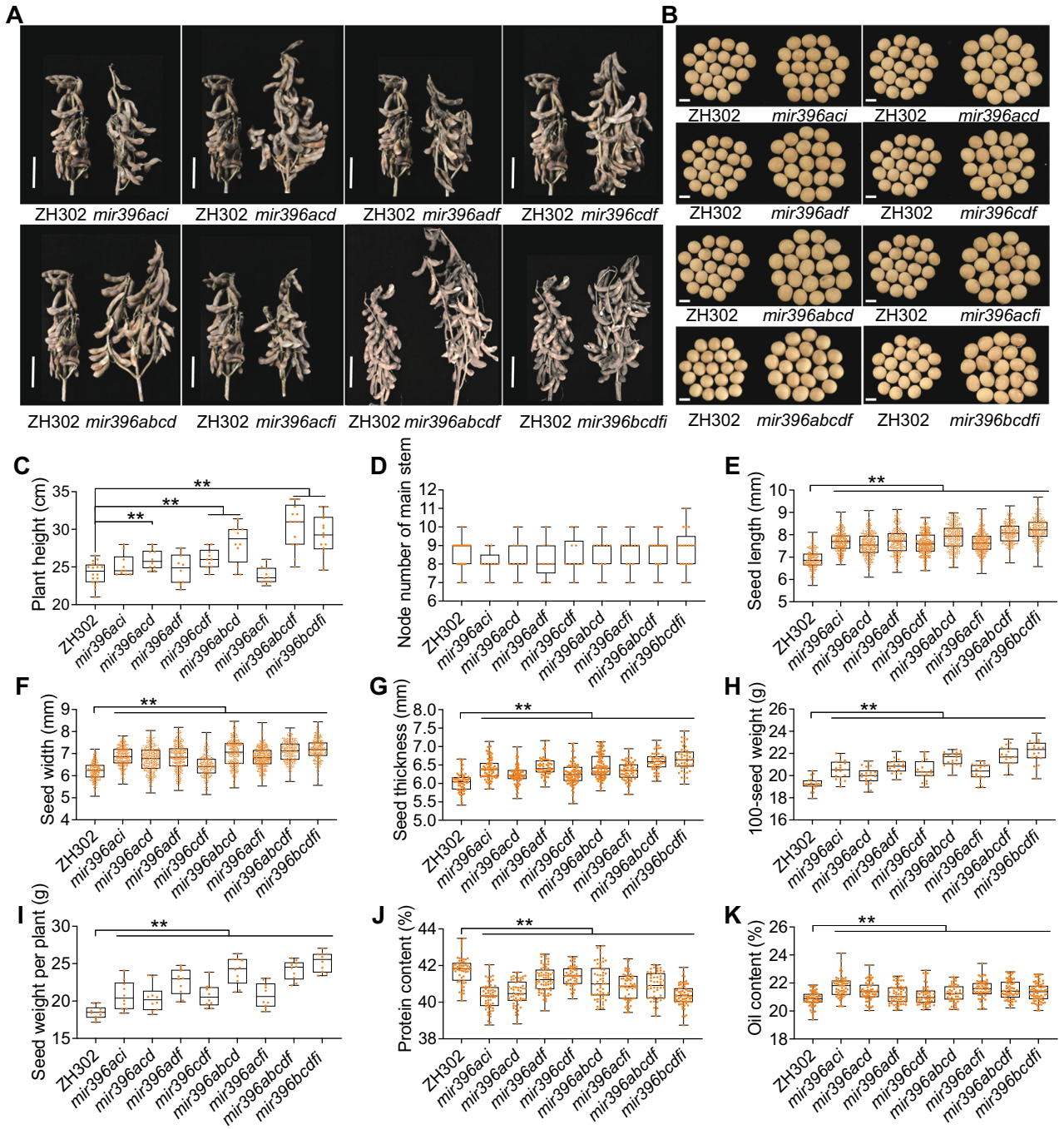

Figure 4. Phenotypic analysis of the *mir396* mutants in Hainan in 2022

(A) Morphology of ZH302 and *mir396* mutants at mature stage. Bar = 5 cm. **(B)** Seeds of ZH302 and *mir396* mutants. Bar = 1 cm. **(C-L)** Quantification of the plant height **(C)**, node number of main stem **(D)**, seed length **(E)**, seed width **(F)**, seed thickness **(G)**, 100-seed weight **(H)**, seed weight per plant **(I)**, seed protein content **(J)** and oil content **(K)** of ZH302 and *mir396* mutants. Data are means ± *SD* (n = 9-23 in **C**, **D**, **H**, and **I**, 120–340 in **E**–**G** and 40–50 in **J**, **K**). Two-tailed Student's *t*-tests were used for statistical analysis. Asterisks indicate significant differences compared with ZH302 (*$P < 0.05$; **$P < 0.01$).

mir396bcdfi mutants are not caused by differences in node number on the main stem. As observed in Shandong Province, all of the *mir396* mutants produced larger and heavier seeds compared to the seeds of ZH302 plants (Figure 4B, I), with an average increase of 13.2%, 10.7%, and 6.3% in seed length, width, and thickness, respectively, resulting in an 8.8% increase in 100-seed weight (Figure 4E–H). Among the mutants, *mir396abcdf* and *mir396bcdfi* exhibited the largest increases in seed length (17.1% and 19.4%), seed width (14.1% and 15.6%), seed thickness (9.9% and 10.3%), and 100-seed weight (13% and 14.8%), respectively. Furthermore, we determined the protein and oil contents in the

mir396 mutant seeds and found that the mutants had less protein but higher oil contents compared to ZH302 seeds (Figure 4J, K). Taken together, these results are consistent with most of the data collected from the *mir396* mutants grown in Shandong Province, with the exception that the two quintuple mutants *mir396abcdf* and *mir396bcdfi* performed much better in Hainan than in Shandong (e.g., the two mutants had increased plant height and yield, and had no lodging problems in Hainan).

Increased expression of *GRF* genes in *mir396abcdf* and *mir396bcdfi* seeds

To explore the effects of the *mir396abcdf* and *mir396bcdfi* mutations on gene expression in soybean, we performed RNA sequencing (RNA-seq) analysis with seeds from *mir396abcdf*, *mir396bcdfi*, and ZH302 at the R6 growth stage when the seeds were still green but fully filled. The RNA-seq results showed that there were 1,947 up-regulated genes and 1,479 down-regulated genes in the *mir396bcdfi* mutant, and 812 up-regulated genes and 676 down-regulated genes in the *mir396abcdf* mutant (Figures 5A, B, S3A; Tables S1, S2). The RNA-seq analysis also indicated that 623 and 473 genes were overlapping up-regulated or down-regulated genes, respectively, for *mir396abcdf* and *mir396bcdfi* (Figure 5A–C). Furthermore, a hierarchical clustering heatmap of the expression of 24 *GRFs* was divided into two clusters. The expression of the 13 cluster 1 *GRFs* was up-regulated in both *mir396abcdf* and *mir396bcdfi* compared with ZH302 (Figure 5D). Among the 24 *GRFs*, it has been shown through miRNA cleavage assays that *GRF6*, *GRF8*, *GRF9*, *GRF10*, *GRF11*, *GRF12*, *GRF13*, *GRF15*, *GRF16*, *GRF17*, and *GRF19* are targets of *miR396* family members in soybean (Noon et al., 2019). We carried out quantitative reverse transcription polymerase chain reaction (qRT-PCR) analysis on some of the *GRFs* and the results indicated that the expression of *GRF1*, *GRF2*, *GRF4*, *GRF8*, *GRF10*, *GRF13*, *GRF14*, *GRF18*, and *GRF23* was increased in the *mir396abcdf* seeds and the expression of *GRF2*, *GRF4*, *GRF8*, *GRF10*, *GRF13*, *GRF14*, *GRF18*, *GRF19*, and *GRF23* was increased in the *mir396bcdfi* seeds (Figure 5E). These results suggest that our RNA-seq data are reliable. Among the deferentially expressed genes in the *mir396abcdf* and *mir396bcdfi* mutants, a large number of them are involved in sugar metabolism, lipid metabolism, and seed development (Figures 5F, S3B–D). The altered expression of the genes in the *mir396abcdf* and *mir396bcdfi* mutants may partially explain the altered plant height and seed size in these two mutants.

DISCUSSION

As an important crop for food, protein, oil and animal feed, the yield and quality of soybean are critical for global food security. Growth and development of soybean is often restricted by the ecological zones of its cultivation. Soybean plants in ecological zones with low latitude tend to flower early in response to the short-day photoperiod, leading to relatively low yield. Because of the variation in photoperiod in natural daylight conditions in the field, the cultivars adapted for high latitude usually perform poorly in lower latitude ecological zones and *vice versa*. Therefore, breeding for soybean varieties with increased yield and better adaptation to grow in broader ecological zones is of vital importance. In this study, we engineered soybean plants with differential adaptation to ecological zones with low latitude and high latitude through precise genome editing of the *miR396* family genes using CRISPR-Cas12SF01. The triple mutants *mir396adf* and *mir396cdf* are suited for the ecological zones with relatively high latitude in the Huang-Huai River region of China, while the quintuple mutants *mir396abcdf* and *mir396bcdfi* are more suited for the ecological zones with lower latitude like the Hainan Island of China. We speculate that additional mutations in *miR396b* and *miR396i* made the quintuple mutants (*mir396abcdf* and *mir396bcdfi*) different from the two triple mutants (*mir396adf* and *mir396cdf*). It is possible that certain *GRFs* targeted by *miR396b* and *miR396i* and other proteins that interact with these GRFs may play an essential role in mediating adaptations to ecological growth conditions.

We observed significant increase in seed size in all of the *mir396* mutants generated in this study: the triple mutants *mir396aci*, *mir396acd*, *mir396adf*, and *mir396cdf*, quadruple mutants *mir396abcd* and *mir396acfi*, and quintuple mutants *mir396abcdf* and *mir396abcdfi* (Figures 2–4). This observation suggests that all of the *miR396* family members are involved in regulating seed size in soybean. We performed RNA-seq analysis with the two quintuple mutants (*mir396abcdf* and *mir396bcdfi*) to explore potential alterations of gene expression when five of the six *miR396* family members are mutated (Figure 5). Our RNA-seq analysis revealed changes in the expression of genes with diverse biological functions including sugar metabolism, seed development and oil metabolism. Consistent with the loss-of-function of *miR396*, the expression of most of the *GRFs* is increased in the two quintuple mutants (*mir396abcdf* and *mir396bcdfi*). Although the precise molecular function of the *miR396-GRFs* module in soybean remains to be elucidated, our work demonstrated a great potential for genome editing of *miR396* genes to improve soybean seed size and yield, and to broaden its growth zones without yield loss.

MATERIALS AND METHODS

Plant materials and growth conditions

The soybean cultivar Zhonghuang 302 (ZH302) was used in this study. Soybean plants were grown in fields in Sanya (Hainan Province, China) from January to May 2022 and in Jinan (Shandong Province, China) during normal soybean-growing seasons (typically from June to October) in 2022 and 2023. When it is necessary, the soybean plants were also

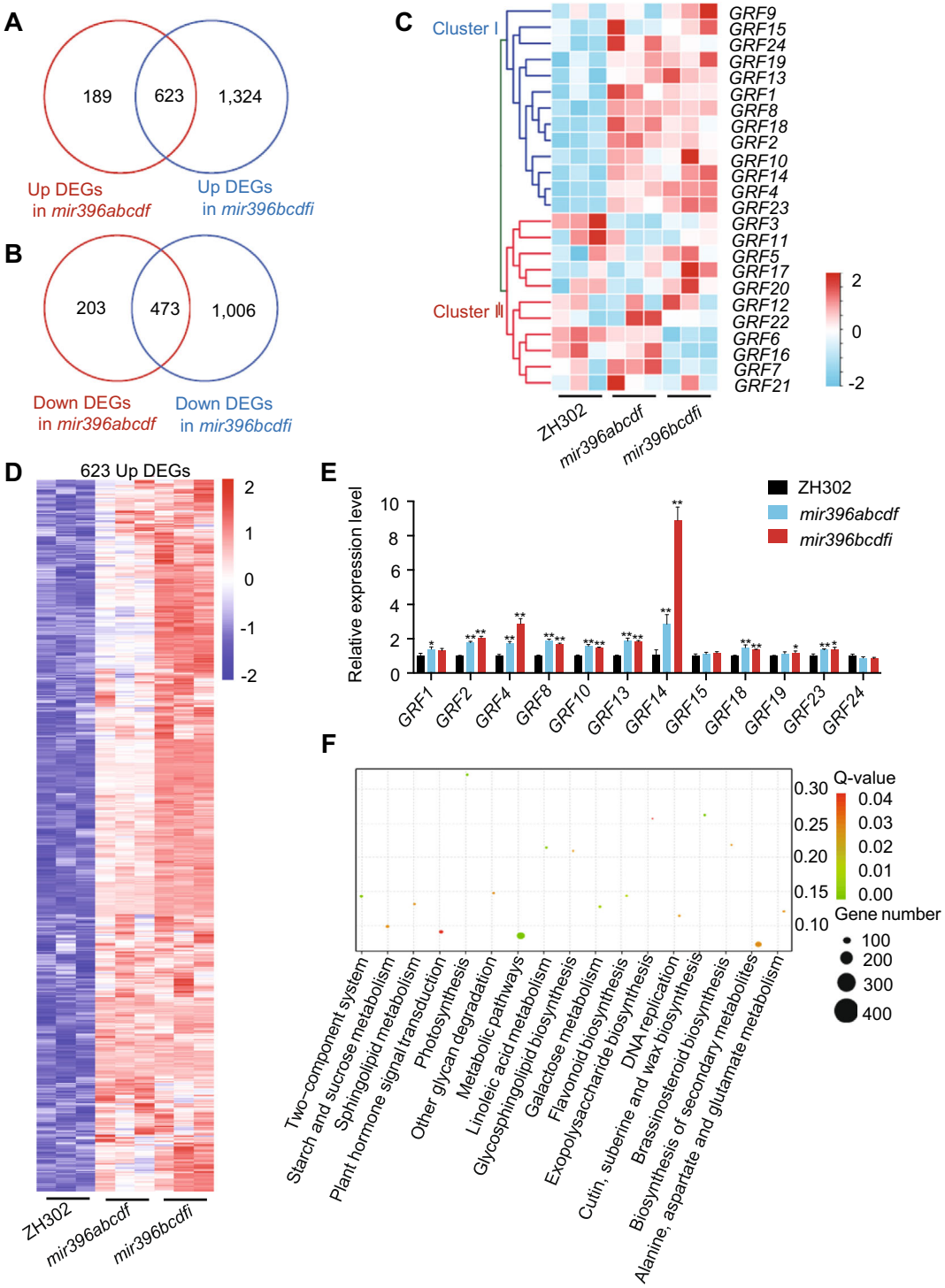

Figure 5. Differentially expressed genes (DEGs) in the seeds of ZH302, *mir396abcdf* and *mir396bcdfi*

(A, B) Overlapping DEGs between *mir396abcdf* and *mir396bcdfi*. **(C)** Heat map of the up DEGs in seeds of ZH302, *mir396abcdf* and *mir396bcdfi*. **(D)** Transcript levels of *GRF1-24* in the *mir396abcdf* and *mir396bcdfi* as determined by RNA-seq analysis. The heat map was conducted using TBtools software (Chen et al., 2020). **(E)** Relative transcript levels of some of the *GRFs* in the ZH302, *mir396abcdf* and *mir396bcdfi*. Values are means ± *SD* ($n = 3$). Two-tailed Student's *t*-tests were used for statistical analysis. Asterisks indicate significant differences compared with ZH302 (*$P < 0.05$; **$P < 0.01$). **(F)** Top 20 of pathway enrichment. The *X*-axis indicates the rich factor corresponding to each pathway, and the *Y*-axis indicates name of the Kyoto Encyclopedia of Genes and Genomes pathway. The color of the point represents the *P*-values of the enrichment analysis. The size and color of bubbles represents the number and degree of enrichment of DEGs, respectively.

cultivated in a growth chamber with a photoperiod of 14 h light (~1,000 μmol m^{-2} s^{-1})/10 h darkness at 25°C.

Vector construction and transformation

The sgRNAs were designed through the online software CRISPR-GE (Xie et al., 2017). The CRISPR/Cas12SF01 binary vector contains the following cassette: *pAtU6*::crRNA1 (harboring DR and sgRNA1 that targets *miR396a* and *miR396i*), *pGmU6*::crRNA2 (harboring DR and sgRNA2 that targets *miR396b*, *miR396c*, *miR396d*, and *miR396f*), *pSlEF1α::Cas12SF01* including the E9t terminator, and in planta selection marker *p35S::BAR*. The binary vector was introduced into *Agrobacterium tumefaciens* (strain EHA105). The soybean *mir396* mutants were generated by the *Agrobacterium tumefaciens*-mediated cotyledon node transformation (Paz et al., 2006) and homozygous *mir396* mutant plants were identified by genotyping PCR reactions and subsequent sequencing of the relevant PCR products. All primers for vector construction and PCR analysis are listed in Table S3.

Measurements of oil content and protein content in soybean seeds

Measurements of oil content and protein content were performed at the Yazhou Bay Seed Lab (Sanya, Hainan, China). Uniform dry seeds of ZH302 and the *mir396* mutants were collected from Hainan and Shandong provinces (China) and measured in a multifunctional near-infrared system (NIRSTM DS 2500F, FOSS, USA) to determine the oil content and protein content. NIRSTM DS 2500F was preheated for at least 30 min before use, and the instrument remained closed during the experiment to ensure the stability of the scan. During spectral acquisition, the uniform dry seeds were evenly distributed in the sample container to ensure that no spaces were generated, which can cause interference of objective factors such as spectral scattering.

DNA and RNA extraction, and RNA-seq and qRT-PCR analyses

Genomic DNA was isolated from leaves at the V2 stage by the cetyltrimethylammonium bromide method as previously described (Mavrodiev et al., 2021).

For RNA-seq analysis, total RNA was extracted from seeds of ZH302, *mir396abcdf* and *mir396bcdfi* plants at the R6 stage. There were three biological replicates. The RNA-seq library preparation and sequencing were performed in Genewiz Company (Suzhou, China). Hisat2(v2.2.1) was used to map the clean data to the soybean reference genome (Williams 82 Assembly 4 Annotation, Wm82.a4.v1). DESeq. 2 (V1.26.0) was used to identify differentially expressed genes (DEGs) with a fold change ≥2 and a false discovery rate <0.05. Gene Ontology (GO) annotation was performed by GOSeq (v1.34.1).

For qRT-PCR analysis, RNA samples from soybean seeds were extracted using FastPure Plant Total RNA Isolation Kit (Catalog No. RC401-01; Vazyme, Nanjing, China). First-stranded complementary DNA (cDNA) was synthesized with PrimeScript RT reagent Kit (Catalog No. RR047A; TaKaRa Biochemical Technology. Beijing, China, and potential genomic DNA contamination in RNA samples was removed by the gDNA Eraser component in this kit prior to cDNA synthesis). Quantitative RT-PCR was performed using SYBR Green I Master Mix on an Applied Biosystems-QuantStudio™ 3 Real-Time PCR System (Thermo Fisher Scientific, Waltham, MA, USA). Gene expression was normalized using the reference gene *GmTubulin* (*β-Tubulin*, *Glyma.17G258300*). The primers used for qRT-PCR are listed in Table S3.

Trait measurement and plot field tests

The seed length and width were measured using an SC-A grain analysis system (Wseen Company, China). The seed thickness was measured by an electronic digital display Vernier caliper. Fully filled grains were used for measuring the 100-seed weight.

In 2022, plants of the ZH302 and *mir396* mutants were grown in fields in Jinan under natural conditions. The area per plot was 15 m^2 with three equal-sized plot replications and six rows were planted in each plot, and the yield was tested with plants collected from the middle four rows. The length of each plot was 6 m, and the row spacing and plant spacing were 40 and 12 cm, respectively. After 3 weeks, the seedlings were manually thinned to achieve an equal density of 14,000 individual plants per 666.7 m^2.

In 2023, plants of the ZH302, *mir396adf* and *mir396abcdf* mutants were grown in fields in Jinan under natural conditions. The area per plot was 150 m^2 and 15 rows were planted in each plot with three equal-sized plot replications. The length of each plot was 25 m, and the row spacing and plant spacing were 40 and 12 cm, respectively. After 3 weeks, the seedlings were manually thinned to achieve an equal density of 14,000 individual plants per 666.7 m^2.

Data availability statement

The RNA-seq data were deposited in the National Center for Biotechnology Information Sequence Read Archive (BioProject: PRJNA1084194).

ACKNOWLEDGEMENTS

This work was supported by Bellagen Biotechnology Inc., and by the National Key Research and Development Program of China (No. NK2022010301), the Seed-Industrialized Development Program in Shandong Province, China (No. 2021LZGC003), the Key Research & Development Program of Shandong Province, China (No. 2021LZGC012), the Innovative research team of Anhui Education (No. 2022AH010056), the National Natural Science Foundation of China (No. 32270367), and the PhD Scientific Research and Innovation Foundation of Sanya Yazhou Bay Science and Technology City (No. HSPHDSRF-2023-11-007).

CONFLICTS OF INTEREST

The authors declare no conflict of interest.

AUTHOR CONTRIBUTIONS

H.X., Q.N., J.-K.Z., and J.Z. contributed to the conceptualization of the project. H.X., F.S., Q.N., L.G., X.C., M. S., J.D., R.G., Y.Z., Y.D., Z.J., and K.P. performed the research. H.X., F.S., Q.N., L.G., Z.Z., J.-K.Z., and J.Z. analyzed the data. H.X., F.S., J.-K.Z., and J.Z. wrote the manuscript. All authors read and approved the contents of this paper.

Edited by: Fanjiang Kong, Guangzhou University, China

Received Jan. 28, 2024; **Accepted** Mar. 22, 2024

OO: OnlineOpen

REFERENCES

Bodirsky, B.L., Rolinski, S., Biewald, A., Weindl, I., Popp, A., and Lotze-Campen, H. (2015). Global food demand scenarios for the 21st century. PLoS ONE **10:** e0139201.

Cai, Z., Xian, P., Cheng, Y., Zhong, Y., Yang, Y., Zhou, Q., Lian, T., Ma, Q., Nian, H., and Ge, L. (2023). MOTHER-OF-FT-AND-TFL1 regulates the seed oil and protein content in soybean. New Phytol. **239:** 905–919.

Che, R., Tong, H., Shi, B., Liu, Y., Fang, S., Liu, D., Xiao, Y., Hu, B., Liu, L., Wang, H., et al. (2015). Control of grain size and rice yield by GL2-mediated brassinosteroid responses. Nat. Plants **2:** 15195.

Chen, C., Chen, H., Zhang, Y., Thomas, H.R., Frank, M.H., He, Y., and Xia, R. (2020). TBtools: An integrative toolkit developed for interactive analyses of big biological data. Mol. Plant **13:** 1194–1202.

Duan, P., Ni, S., Wang, J., Zhang, B., Xu, R., Wang, Y., Chen, H., Zhu, X., and Li, Y. (2015). Regulation of OsGRF4 by OsmiR396 controls grain size and yield in rice. Nat. Plants **2:** 15203.

Duan, Z., Liang, Y., Sun, J., Zheng, H., Lin, T., Luo, P., Wang, M., Liu, R., Chen, Y., Guo, S., et al. (2024). An engineered Cas12i nuclease that is an efficient genome editing tool in animals and plants. The Innovation **5:** 100564.

Gao, F., Wang, K., Liu, Y., Chen, Y., Chen, P., Shi, Z., Luo, J., Jiang, D., Fan, F., Zhu, Y., et al. (2016). Blocking miR396 increases rice yield by shaping inflorescence architecture. Nat. Plants **2:** 15196.

He, L., and Hannon, G.J. (2004). MicroRNAs: Small RNAs with a big role in gene regulation. Nat. Rev. Genet. **5:** 522–531.

Hu, J., Wang, Y., Fang, Y., Zeng, L., Xu, J., Yu, H., Shi, Z., Pan, J., Zhang, D., Kang, S., et al. (2015). A rare allele of GS2 enhances grain size and grain yield in rice. Mol. Plant **8:** 1455–1465.

Hu, Y., Liu, Y., Lu, L., Tao, J.-J., Cheng, T., Jin, M., Wang, Z.-Y., Wei, J.-J., Jiang, Z.-H., Sun, W.-C., et al. (2023a). Global analysis of seed transcriptomes reveals a novel PLATZ regulator for seed size and weight control in soybean. New Phytol. **240:** 2436–2454.

Hu, Y., Liu, Y., Tao, J.-J., Lu, L., Jiang, Z.-H., Wei, J.-J., Wu, C.-M., Yin, C.-C., Li, W., Bi, Y.-D., et al. (2023b). GmJAZ3 interacts with GmRR18a and GmMYC2a to regulate seed traits in soybean. J. Integr. Plant Biol. **65:** 1983–2000.

Jones-Rhoades, M.W., Bartel, D.P., and Bartel, B. (2006). MicroRNAS and their regulatory roles in plants. Annu. Rev. Plant Biol. **57:** 19–53.

Li, S., Gao, F., Xie, K., Zeng, X., Cao, Y., Zeng, J., He, Z., Ren, Y., Li, W., Deng, Q., et al. (2016). The OsmiR396c-OsGRF4-OsGIF1 regulatory module determines grain size and yield in rice. Plant Biotechnol. J. **14:** 2134–2146.

Liu, J.-Y., Zhang, Y.-W., Han, X., Zuo, J.-F., Zhang, Z., Shang, H., Song, Q., and Zhang, Y.-M. (2020). An evolutionary population structure model reveals pleiotropic effects of GmPDAT for traits related to seed size and oil content in soybean. J. Exp. Bot. **71:** 6988–7002.

Lv, P., Su, F., Chen, F., Yan, C., Xia, D., Sun, H., Li, S., Duan, Z., Ma, C., Zhang, H., et al. (2024). Genome editing in rice using CRISPR/Cas12i3. Plant Biotechnol. J. **22:** 379–385.

Mavrodiev, E.V., Dervinis, C., Whitten, W.M., Gitzendanner, M.A., Kirst, M., Kim, S., Kinser, T.J., Soltis, P.S., and Soltis, D.E. (2021). A new, simple, highly scalable, and efficient protocol for genomic DNA extraction from diverse plant taxa. Appl. Plant Sci. **9:** e11413.

Miao, C., Wang, D., He, R., Liu, S., and Zhu, J.-K. (2020). Mutations in MIR396e and MIR396f increase grain size and modulate shoot architecture in rice. Plant Biotechnol. J. **18:** 491–501.

Noon, J.B., Hewezi, T., Baum, T.J. (2019). Homeostasis in the soybean miRNA396-GRF network is essential for productive soybean cyst nematode infections. J. Exp. Bot. **70:** 1653–1668.

Paz, M.M., Martinez, J.C., Kalvig, A.B., Fonger, T.M., and Wang, K. (2006). Improved cotyledonary node method using an alternative explant derived from mature seed for efficient Agrobacterium-mediated soybean transformation. Plant Cell Rep. **25:** 206–213.

Tang, X., Su, T., Han, M., Wei, L., Wang, W., Yu, Z., Xue, Y., Wei, H., Du, Y., Greiner, S., et al. (2017). Suppression of extracellular invertase inhibitor gene expression improves seed weight in soybean (*Glycine max*). J. Exp. Bot. **68:** 469–482.

Van Daele, I., Gonzalez, N., Vercauteren, I., de Smet, L., Inzé, D., Roldán-Ruiz, I., and Vuylsteke, M. (2012). A comparative study of seed yield parameters in *Arabidopsis thaliana* mutants and transgenics. Plant Biotechnol. J. **10:** 488–500.

Wang, S., Liu, S., Wang, J., Yokosho, K., Zhou, B., Yu, Y.-C., Liu, Z., Frommer, W.B., Ma, J.-F., Chen, L.-Q., et al. (2020). Simultaneous changes in seed size, oil content and protein content driven by selection of SWEET homologues during soybean domestication. Natl. Sci. Rev. **7:** 1776–1786.

Xie, X., Ma, X., Zhu, Q., Zeng, D., Li, G., and Liu, Y.-G. (2017). CRISPR-GE: A convenient software toolkit for crispr-based genome editing. Mol. Plant **10:** 1246–1249.

Xing, Y., and Zhang, Q. (2010). Genetic and molecular bases of rice yield. Annu. Rev. Plant Biol. **61:** 421–442.

Zhang, J., Zhou, Z., Bai, J., Tao, X., Wang, L., Zhang, H., and Zhu, J.-K. (2020). Disruption of MIR396e and MIR396f improves rice yield under nitrogen-deficient conditions. Natl. Sci. Rev. **7:** 102–112.

SUPPORTING INFORMATION

Additional Supporting Information may be found online in the supporting information tab for this article: http://onlinelibrary.wiley.com/doi/10.1111/jipb.13660/suppinfo

Figure S1. Predicted stem-loop structures of the *Gma-miR396* gene family

Figure S2. Sanger sequencing of the *mir396* mutants

Figure S3. Deferentially expressed genes in *mir396abcdf* and *mir396bcdfi*

Table S1. Genes with altered expression in mir396bcdfi as determined by RNA sequencing analysis

Table S2. Genes with altered expression in mir396abcdf as determined by RNA sequencing analysis

Table S3. Primers used in this study

Scan using WeChat with your smartphone to view JIPB online

Scan with iPhone or iPad to view JIPB on Twitter